Inorganic Chemistry

Article

pubs.acs.org/IC

Synthesis and Coordination Behavior of a Bipyridine Platinum(II) Complex with Thioglucose

Takaaki Tsuji, Naoto Kuwamura, Nobuto Yoshinari, and Takumi Konno*

Department of Chemistry, Graduate School of Science, Osaka University, Toyonaka, Osaka 560-0043, Japan

Supporting Information

ABSTRACT: A mononuclear platinum(II) complex with two monodentate-*S* H_4tg^- ligands, $[Pt(H_4tg\text{-}\kappa S)_2(bpy)]$ (**1**), was newly synthesized by the reaction of $[PtCl_2(bpy)]$ (bpy = 2,2′-bipyridyl) with NaH_4tg (NaH_4tg =1-thio-β-D-glucose sodium salt) in water. Complex **1** reacted with additional $[PtCl_2(bpy)]$ in water to give an S-bridged dinuclear complex, $[Pt_2(\mu_2\text{-}H_4tg\text{-}\kappa^1S{:}\kappa^1S)_2(bpy)_2]^{2+}$ ($[\mathbf{2}]^{2+}$), in which a square-planar $[Pt(H_4tg)_2(bpy)]$ unit binds to a $[Pt(bpy)]^{2+}$ moiety through two thiolato groups. Treatments of **1** with Cu^{2+} and Ni^{2+} in water in the presence of bpy produced S-bridged dinuclear complexes $[PtCu(\mu_2\text{-}H_4tg\text{-}\kappa^1S{:}\kappa^2O,S)_2(bpy)_2]^{2+}$ ($[\mathbf{3}]^{2+}$) and $[PtNi(\mu_2\text{-}H_4tg\text{-}\kappa^1S{:}\kappa^2O,S)_2(bpy)_2]^{2+}$ ($[\mathbf{4}]^{2+}$), respectively, in which a square-planar $[Pt(H_4tg)_2(bpy)]$ unit binds to a $[M(bpy)]^{2+}$ (M = Cu^{II}, Ni^{II}) moiety through two thiolato and two hydroxyl groups to form a chiral $[M(N)_2(O)_2(S)_2]$ octahedron with the Δ configuration. On the other hand, similar treatment with Cd^{2+} in the presence of bpy resulted in the formation of an S-bridged trinuclear complex, $[Cd\{Pt(\mu_2\text{-}H_4tg\text{-}\kappa^1S{:}\kappa^2O,S)(\mu_2\text{-}H_4tg\text{-}\kappa^1S{:}\kappa^1S)(bpy)\}_2]^{2+}$ ($[\mathbf{5}]^{2+}$), in which each of two square-planar $[Pt(H_4tg)_2(bpy)]$ units binds to a Cd^{II} ion through two thiolato groups and one hydroxyl group to form a chiral $[Cd(O)_2(S)_4]$ octahedron with the Λ configuration. Of two geometrical configurations, syn and anti, which arise from the relative arrangement of two β-D-pyranose moieties, $[\mathbf{2}]^{2+}$ adopts the syn configuration with symmetric bridging sulfur atoms, while $[\mathbf{3}]^{2+}$, $[\mathbf{4}]^{2+}$, and $[\mathbf{5}]^{2+}$ all have the anti configuration with *R* configurational bridging sulfur atoms. All of the complexes were fully characterized by electronic absorption, CD, and NMR spectroscopies, along with single-crystal X-ray crystallography.

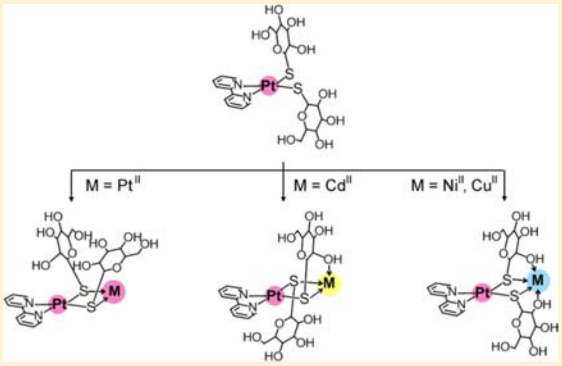

INTRODUCTION

1-Thio-β-D-glucose (H_5tg = $C_6H_{12}O_5S$) is one of the simplest thiol-containing hexoses.[1] It has been used as starting material for a variety of synthetic *S*-glycosides in organic chemistry and as a coating reagent for gold nanoparticles and electrodes in material science.[1−3] In coordination chemistry, the development of transition-metal complexes with H_5tg was initially motivated by the finding that some Au^I−thiolate compounds show an antirheumatoid activity.[4] During the late 1920s, Landé and Pick independently reported that aurothioglucose ($[Au(H_4tg\text{-}S)]_n$) has an effect on rheumatic disease.[5a,b] The subsequent studies established an excellent antirheumatoid activity for this complex, which has been attributed to its hydrophilicity and the biocompatibility of the sugar backbone.[4,5] The investigation of this class of complexes was extended to include a phosphine compound as a coligand, and a number of related Au^I complexes, such as $[Au(H_4tg\text{-}S)(PEt_3)]$, $[Au_2(H_4tg\text{-}S)_2(dppe)]$ (dppe = 1,2-bis(diphenylphosphino)ethane), and $[Au(Ac_4tg\text{-}S)(PEt_3)]$ (auranofin), were prepared and their antirheumatoid activities were studied.[4,6] On the other hand, reports on the synthesis of coordination compounds from H_5tg in combination with a transition-metal ion other than Au^I are relatively limited,[7−10] despite the presence of both soft thiol and hard hydroxyl groups in H_5tg available for coordination to a variety of metal centers. In particular, only a few transition-metal complexes that are fully characterized have been presented to date,[8] and to the best of our knowledge, $[Co(H_3tg\text{-}S,O)(en)_2]^+$ (en = ethylenediamine) and $[ReO(SSS)(H_4tg\text{-}S)]$ (SSS = 2,2′-thiodiethanethiolate) are the only transition-metal complexes that have been structurally characterized by single-crystal X-ray crystallography.[9,10] This is most likely because of the significant hydrophilicity of glycosyl moiety in H_5tg, which makes it difficult to isolate target species in a pure form from a reaction mixture in solution.[11]

As part of our continuing interest in chiral coordination compounds having thiolato donor groups, which potentially function as an S-donating chiral metalloligand,[12−16] we started to investigate the rational preparation of an inert thiolato platinum(II) system by using H_5tg as a chiral ligand. Our strategy is the introduction of a hydrophobic diimine-type coligand in a platinum(II) coordination system, which should compensate the hydrophilicity of glycosyl moieties to facilitate the isolation and crystallization of a platinum(II) complex from the polar reaction medium that is required to dissolve H_5tg. In this study, we employed 2,2′-bipyridyl (bpy) as a diimine-type

Received: February 4, 2013
Published: April 11, 2013

Scheme 1. Synthetic routes for [1] and $[2]^{2+}$

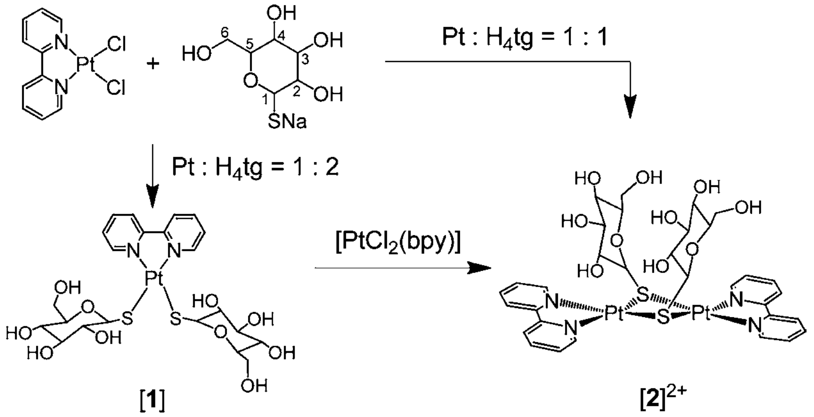

Scheme 2. Synthetic routes for $[3]^{2+}$, $[4]^{2+}$, and $[5]^{2+}$

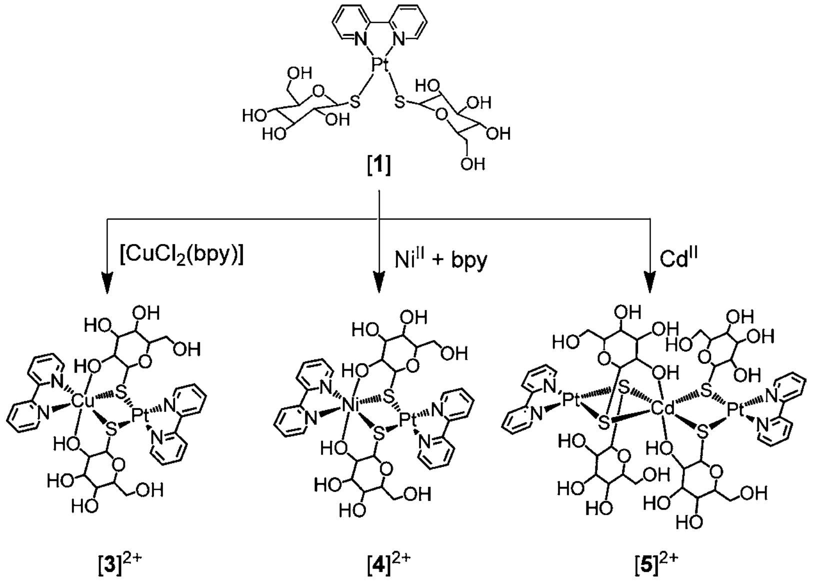

coligand. This ligand is expected to show intermolecular π–π interactions that also contribute to decrease the solubility of a platinum(II) complex in a polar solvent.[17] Indeed, we were able to isolate a new transition-metal complex with two H_4tg^- ligands, $[Pt(H_4tg\text{-}S)_2(bpy)]$ ([1]), by a simple 1:2 reaction of $[PtCl_2(bpy)]$ and H_4tg^- in water (Scheme 1). Furthermore, [1] was found to react with a second transition-metal ion (M = Pt^{II}, Cu^{II}, Ni^{II}, Cd^{II}), giving S-bridged dinuclear or trinuclear complexes with retention of the mononuclear structure in [1] (Scheme 2). In this paper, we report on the synthesis and characterization of these new coordination compounds containing H_4tg^- ligand. Notably, all four dinuclear or trinuclear complexes obtained were structurally characterized by single-crystal X-ray diffraction. This study demonstrates the functionality of [1] as a versatile chiral metalloligand available for the chiralselective construction of S-bridged multinuclear structures, as well as the effectiveness of the introduction of a diimine-type coligand to isolate coordination compounds with hydrophilic glycosyl moieties.

■ EXPERIMENTAL SECTION

Preparation of $[Pt(H_4tg\text{-}\kappa S)_2(bpy)]$ (1). To a yellow suspension of $[PtCl_2(bpy)]$[18] (0.50 g, 1.18 mmol) in water (300 mL) was added a solution of NaH_4tg (0.59 g, 2.70 mmol) in water (20 mL). The mixture was stirred at 60 °C for 1 h to give an orange solution. After a small amount of unreacted $[PtCl_2(bpy)]$ was filtered off, the filtrate was evaporated to dryness using a rotary evaporator. The orange residue was dissolved in 20 mL of water, followed by allowing it to stand at room temperature overnight. The resulting orange, fiberous product was collected by filtration. Yield: 0.75 g (81%). Anal. Calcd for $[Pt(H_4tg\text{-}\kappa S)_2(bpy)]\cdot 2H_2O$ ($[1]\cdot 2H_2O$ = $C_{22}H_{34}N_2O_{12}PtS_2$): C, 33.98; H, 4.41; N, 3.60. Found: C, 33.82; H, 4.26; N, 3.59. ^1H NMR (D_2O): δ 9.54 (2H, d, J = 4.9 Hz, bpy), 8.29 (2H, d, J = 7.6 Hz, bpy), 8.22 (2H, t, J = 7.8 Hz, bpy), 7.66 (2H, t, 6.7 Hz, bpy), 3.82 (2H, d, J = 12.2 Hz, H_4tg^-), 3.62 (1H, d, J = 6.1 Hz, H_4tg^-), 3.59 (1H, d, J = 5.9 Hz, H_4tg^-), 3.51–3.34 (10H, m, H_4tg^-).

Preparation of $[Pt_2(\mu_2\text{-}H_4tg\text{-}\kappa^1S{:}\kappa^1S)_2(bpy)_2](ClO_4)_2$ ($[2](ClO_4)_2$). *Method A.* To an orange suspension of $[1]\cdot 2H_2O$ (0.05 g, 0.06 mmol) in water (50 mL) was added a solid sample of $[PtCl_2(bpy)]$ (0.03 g, 0.07 mmol). The mixture was stirred at 50 °C for 2.5 h to give a yellow-brown solution. After a small amount of unreacted $[PtCl_2(bpy)]$ was filtered off, the filtrate was concentrated to dryness using a rotary evaporator. The yellow green residue was dissolved in 10 mL of water, and an aqueous $NaClO_4$ solution (0.5 mL, 5 M) was added to it. The solution was allowed to stand at room temperature for 10 days. The resulting yellow block crystals were collected by filtration. Yield: 0.06 g (64%). One of the crystals thus obtained was used for X-ray analysis. Anal. Calcd for $[Pt_2(\mu_2\text{-}H_4tg\text{-}\kappa^1S{:}\kappa^1S)_2(bpy)_2](ClO_4)_2\cdot 9H_2O$ ($[2](ClO_4)_2\cdot 9H_2O$ = $C_{32}H_{56}N_4Cl_2O_{27}Pt_2S_2$): C, 26.43; H, 3.88; N, 3.85. Found: C, 26.37; H, 3.69; N, 3.89. ^1H NMR (D_2O): δ 8.92 (d, 2H, J = 5.65 Hz, bpy), 8.77 (d, 2H, J = 5.34 Hz, bpy), 8.23 (t, 4H, J = 7.55 Hz, bpy), 8.10 (d, 4H, J = 8.09 Hz, bpy), 7.80 (t, 2H, J = 6.48 Hz, bpy), 7.74 (t, 2H, J = 6.48 Hz, bpy), 5.03 (d, 2H, J = 9.16 Hz, H_4tg^-), 3.41−3.23 (m, 12H, H_4tg^-). $^{13}C\{^1H\}$ NMR (D_2O): δ 157.5 (bpy), 157.4 (bpy), 151.0 (bpy), 150.2 (bpy), 144.8 (bpy), 144.7 (bpy), 130.6 (bpy), 130.5 (bpy), 126.7 (bpy), 126.5 (bpy), 86.56 (H_4tg^-), 83.07 (H_4tg^-), 79.61 (H_4tg^-), 76.81 (H_4tg^-), 71.30 (H_4tg^-), 62.76 (H_4tg^-). ESI-MS (in MeOH) m/z: 546.1 ($[M]^{2+}$).

Method B. To a yellow suspension of $[PtCl_2(bpy)]$ (0.10 g, 0.24 mmol) in water (60 mL) was added a solution of NaH_4tg (0.06 g, 0.27 mmol) in water (5 mL). The mixture was stirred at 50 °C for 3 h to give a yellow solution. After a small amount of unreacted $[PtCl_2(bpy)]$ was filtered off, the filtrate was concentrated to ca. 20 mL using a rotary evaporator. An aqueous $NaClO_4$ solution (0.5 mL, 5 M) was added to the yellow concentrated solution, followed by allowing it to stand at room temperature for 5 days. The resulting yellow block crystals of $[\mathbf{2}](ClO_4)_2\cdot 9H_2O$ were collected by filtration. Yield: 0.12 g (70%).

Preparation of $[PtCu(\mu_2\text{-}H_4tg\text{-}\kappa^1S{:}\kappa^2O,S)_2(bpy)_2](NO_3)_2$ ($[\mathbf{3}](NO_3)_2$). To a suspension of $[\mathbf{1}]\cdot 2H_2O$ (0.05 g, 0.06 mmol) in water (10 mL) was added a solution of $[CuCl_2(bpy)]$[19] (0.02 g, 0.07 mmol) in water (5 mL). The mixture was stirred at room temperature for 1 h, and an aqueous $NaNO_3$ solution (1 mL, 5 M) was added to it. The solution was allowed to stand at room temperature for 2 days to give green block crystals, which were collected by filtration and washed with a small amount of water. Yield: 0.04 g (55%, based on Pt). Anal. Calcd for $[PtCu(\mu_2\text{-}H_4tg\text{-}\kappa^1S{:}\kappa^2O,S)_2(bpy)_2](NO_3)_2\cdot 2H_2O$ ($[\mathbf{3}](NO_3)_2\cdot 2H_2O$ = $C_{32}H_{42}N_6CuO_{18}PtS_2$): C, 34.27; H, 3.77; N, 7.49. Found: C, 34.29; H, 3.69; N, 7.50.

Single crystals of $[\mathbf{3}](ClO_4)_2\cdot 2H_2O$ used for X-ray analysis were obtained by the following method: To a suspension of $[PtCl_2(bpy)]$ (0.08 g, 0.19 mmol) in water (10 mL) was added a solution of NaH_4tg (0.09 g, 0.41 mmol) in water (2 mL). The mixture was stirred at room temperature for 4 h to give an orange suspension, to which a solution of $[CuCl_2(bpy)]$ (0.06 g, 0.21 mmol) in 5 mL of water was added. The mixture was stirred at room temperature for 2 h to give a green suspension. After insoluble materials were filtered off, to the green filtrate was added a small amount of saturated $NaClO_4$ aqueous solution. The solution was allowed to stand at room temperature for 3 days to give green block crystals of $[\mathbf{3}](ClO_4)_2\cdot 2H_2O$.

Preparation of $[PtNi(\mu_2\text{-}H_4tg\text{-}\kappa^1S{:}\kappa^2O,S)_2(bpy)_2](NO_3)_2$ ($[\mathbf{4}](NO_3)_2$). To a suspension of $[\mathbf{1}]\cdot 2H_2O$ (0.05 g, 0.06 mmol) in water (10 mL) was added a solution of $Ni(NO_3)_2\cdot 6H_2O$ (0.02 g, 0.07 mmol) in water (2 mL). The mixture was stirred at 40 °C for 1 h to give a yellowish brown solution. A solid sample of bpy (0.01 g, 0.06 mmol) was added to it, and the mixture was stirred at 40 °C for 2 h to give a yellow-brown solution. To this reaction solution was added an aqueous $NaNO_3$ solution (1 mL, 5 M), followed by allowing it to stand at room temperature for 12 days. The resulting pale green crystals were collected by filtration and washed with a small amount of water. One of the crystals thus obtained was used for X-ray analysis. Yield: 0.04 g (57%, based on Pt). Anal. Calcd for $[PtNi(\mu_2\text{-}H_4tg\text{-}\kappa^1S{:}\kappa^2O,S)_2(bpy)_2](NO_3)_2\cdot H_2O$ ($[\mathbf{4}](NO_3)_2\cdot H_2O$ = $C_{32}H_{40}N_6NiO_{17}PtS_2$): C, 34.99; H, 3.67; N, 7.65. Found: C, 34.74; H, 3.68; N, 7.69.

Preparation of $[Cd\{Pt(\mu_2\text{-}H_4tg\text{-}\kappa^1S{:}\kappa^2O,S)(\mu_2\text{-}H_4tg\text{-}\kappa^1S{:}\kappa^1S)(bpy)\}_2](ClO_4)_2$ ($[\mathbf{5}](ClO_4)_2$). *Method A.* To an orange suspension of $[\mathbf{1}]\cdot 2H_2O$ (0.025 g, 0.03 mmol) in water (5 mL) was added a solution of $CdCl_2\cdot 2.5H_2O$ (0.008 g, 0.04 mmol) in water (1 mL). The mixture was stirred at 40 °C for 2 h to give a yellow solution. A solid sample of bpy (0.005 g, 0.03 mmol) was added to it, and the mixture was stirred at 40 °C for 1 h to give a yellow suspension. After a small amount of colorless solid was filtered off, to the yellow filtrate was added an aqueous $NaClO_4$ solution (10 drops, 1 M). The solution was allowed to stand at room temperature for 5 days. The resulting yellow block crystals were collected by filtration and washed with a small amount of water. Yield: 0.005 g (16%, based on Pt). Anal. Calcd for $[Cd\{Pt(\mu_2\text{-}H_4tg\text{-}\kappa^1S{:}\kappa^2O,S)(\mu_2\text{-}H_4tg\text{-}\kappa^1S{:}\kappa^1S)(bpy)\}_2](ClO_4)_2\cdot 6H_2O$ ($[\mathbf{5}](ClO_4)_2\cdot 6H_2O$ = $C_{44}H_{72}N_4CdCl_2O_{34}Pt_2S_4$): C, 27.77; H, 3.81; N, 2.94. Found: C, 27.88; H, 3.70; N, 2.95.

Method B. To a suspension of $[\mathbf{1}]\cdot 2H_2O$ (0.05 g, 0.06 mmol) in water (10 mL) was added a solution of $CdBr_2$ (0.009 g, 0.03 mmol) in water (2 mL). The mixture was stirred at room temperature for 15 min to give a yellow solution. To this solution was added an aqueous $NaClO_4$ solution (8 drops, 5 M), followed by allowing it to stand at room temperature for 6 days. The resulting yellow block crystals of $[\mathbf{5}](ClO_4)_2\cdot 6H_2O$ were collected by filtration. One of the crystals thus obtained was used for X-ray analysis. Yield: 0.044 g (72%, based on Pt).

Caution! *Perchlorate salts of metal complexes are potentially explosive and should be handled with great care.*

Measurements. The electronic absorption spectra were recorded with a JASCO Ubest-55, V-570, or V-660 spectrophotometer, and the CD spectra were recorded with a JASCO J-820, J-700, or J-600 spectrophotometer at room temperature. The diffuse reflection spectra in the solid state were recorded on a JASCO V-570 spectrophotometer using $MgSO_4$. The IR spectra were measured with a JASCO FT/IR-550 infrared spectrophotometer using KBr disks. The ^1H and $^{13}C\{^1H\}$ NMR spectra were recorded with a JEOL EX-270 or a GSX-500 spectrometer at the probe temperature in D_2O. Sodium 4,4-dimethyl-4-silapentane-1-sulfonate (DSS) was used as the internal reference. Elemental analyses (C, H, N) were performed with a Yanaco CHN Corder MT-5. The X-ray fluorescence analyses were made on a HORIBA MESA-500 spectrometer. The molar conductivities were measured with a HORIBA DS12 conductivity meter. Electrospray-ionization (ESI) mass spectra were recorded in a positive ion mode on an ABsciex QSTAR Elite controlled by the Analyst QS 2.0 software package. The data of electronic absorption, CD, IR, and ^1H NMR spectra together with molar conductivity are summarized in Tables S6 and S7 of the Supporting Information.

X-ray Structure Determinations. Single-crystal X-ray diffraction measurements for $[\mathbf{2}](ClO_4)_2\cdot 9H_2O$, $[\mathbf{4}](NO_3)_2\cdot 2H_2O$, and $[\mathbf{5}](ClO_4)_2\cdot 6H_2O$ were made on a Rigaku RAXIS RAPID imaging plate diffractometer with graphite-monochromated Mo Kα radiation (λ = 0.7107 Å) at 293, 200, and 200 K, respectively. Unit cell parameters were determined by a least-squares refinement. The intensity data were collected by the ω scan mode up to $2\theta_{max}$ = 54.94° for $[\mathbf{2}](ClO_4)_2\cdot 9H_2O$, to $2\theta_{max}$ = 54.98° for $[\mathbf{4}](NO_3)_2\cdot 2H_2O$, and to $2\theta_{max}$ = 54.96° for $[\mathbf{5}](ClO_4)_2\cdot 6H_2O$. Empirical absorption corrections were also applied. The 10 740, 8915, and 7149 independent reflections with $I > 2\sigma(I)$ of the measured 23 133, 29 367, and 40 029 reflections were considered as "observed" and used for the structure determinations of $[\mathbf{2}](ClO_4)_2\cdot 9H_2O$, $[\mathbf{4}](NO_3)_2\cdot 2H_2O$, and $[\mathbf{5}](ClO_4)_2\cdot 6H_2O$, respectively. The structures were solved by the direct method with SHELXS-97 and expanded using Fourier techniques.[20] The non-hydrogen atoms except oxygen atoms of water and ClO_4^- molecules were refined anisotropically by full-matrix least-squares techniques on F^2 using SHELXL-97.[20] The asymmetric unit contained half of a complex-cation for $[\mathbf{5}](ClO_4)_2\cdot 6H_2O$. In $[\mathbf{2}](ClO_4)_2\cdot 9H_2O$ and $[\mathbf{5}](ClO_4)_2\cdot 6H_2O$, one of two 1-thio-$\beta$-D-glucose moieties was disordered over two positions {$[\mathbf{2}](ClO_4)_2\cdot 9H_2O$, C32A−O10A and C32B−O10B; $[\mathbf{5}](ClO_4)_2\cdot 6H_2O$, C12A-O10A and C12B−O10B}. Several solvated water molecules in $[\mathbf{5}](ClO_4)_2\cdot 6H_2O$ were disordered.

A single-crystal X-ray diffraction measurement for $[\mathbf{3}](ClO_4)_2\cdot 2H_2O$ was made on a Rigaku AFC-7R four-cycle diffractometer with graphite-monochromated Mo Kα radiation at room temperature. The intensity data were collected by the $\omega-2\theta$ scan mode up to $2\theta_{max}$ = 55.08°. The intensities were corrected for Lorentz and polarization effects. Empirical absorption correction based on Ψ scans was also applied. The 5593 independent reflections with $I > 2\sigma(I)$ of the measured 5593 reflections were considered as "observed" and used for the structure determination. The structure was solved by the direct method with SHELXS-97 and expanded using Fourier techniques.[20] The non-hydrogen atoms except oxygen and chlorine atoms of water and ClO_4^- molecules were refined anisotropically by full-matrix least-squares techniques on F^2 using SHELXL-97.[20] Several solvated water molecules in $[\mathbf{3}](ClO_4)_2\cdot 2H_2O$ were disordered.

All calculations were performed using the Crystal Structure crystallographic software package and SHELXL-97 program. Hydrogen atoms except those of water molecules were located at calculated positions and refined as riding models.

The selected bond distances and angles of [**2**]$(ClO_4)_2 \cdot 9H_2O$, [**3**]$(ClO_4)_2 \cdot 2H_2O$, [**4**]$(NO_3)_2 \cdot 2H_2O$, and [**5**]$(ClO_4)_2 \cdot 6H_2O$, as well as their crystallographic data, are summarized in the Supporting Information (Tables S1–S5).

■ RESULTS AND DISCUSSION

Synthesis and Characterization of [Pt(H_4tg-*κS*)$_2$(bpy)] ([1]). The reaction of [$PtCl_2$(bpy)] with NaH_4tg in a 1:2 ratio in water gave an orange solution, from which an orange, fiberous product ([**1**]) was isolated in a good yield. The elemental analytical data of [**1**] were consistent with the formula for [Pt(H_4tg)$_2$(bpy)], and its neutral charge was implied by the molar conductivity in water (3.7 S cm^2 mol^{-1}). The presence of H_4tg^- and bpy ligands in [**1**] in a 2:1 ratio was indicated by its ^1H NMR spectrum in D_2O (Supporting Information, Figure S1), which shows aliphatic proton signals (δ 3.3–3.8) and aromatic proton signals (δ 7.6–9.6) in an integration ratio of 7:4. The electronic absorption spectrum of [**1**] in water shows an intense visible band at 392 nm ($\varepsilon = 2.44 \times 10^3$ M^{-1} cm^{-1}), besides a more intense near-UV band at 298 nm ($\varepsilon = 1.21 \times 10^4$ M^{-1} cm^{-1}) that is typical for a bpy π–π* transition (Figure 1 and Supporting Information, Table S6).[21]

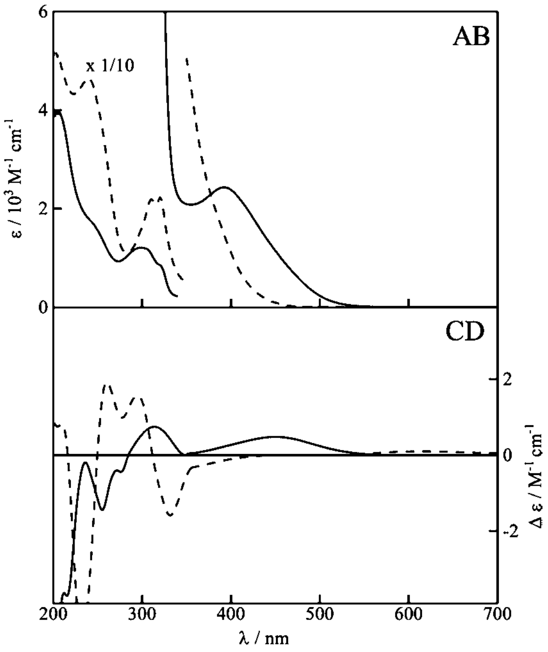

Figure 1. Absorption and CD spectra of [**1**] (solid line) and [**2**]$(ClO_4)_2$ (dashed line) in H_2O.

The visible band is reminiscent of the thiolato-to-diimine charge transfer (LL′CT) band observed for related [Pt(diimine)(thiolato)$_2$]-type complexes.[21c,22] From these results, [**1**] is assigned to a mononuclear platinum(II) complex, [Pt(H_4tg-*κS*)$_2$(bpy)], which contains two monodentate-*S* H_4tg^- ligands. Compatible with the presence of H_4tg^- ligands, [**1**] is optically active, showing positive CD bands in the LL′CT and π–π* transition regions (Figure 1).

Synthesis and Characterization of [Pt_2(μ_2-H_4tg-κ^1S:κ^1S)$_2$(bpy)$_2$]$^{2+}$ ([2]$^{2+}$). To investigate the functionality of [**1**] as an S-donating metalloligand, the reaction of [**1**] with [$PtCl_2$(bpy)] was carried out. When [**1**] was treated with 1 molar equiv of [$PtCl_2$(bpy)] in water, the orange suspension turned to a yellow-brown solution, from which yellow crystals ([**2**]$(ClO_4)_2$) were isolated in a satisfactory yield by the addition of an aqueous solution of $NaClO_4$. The elemental analytical data of [**2**]$(ClO_4)_2$ were in agreement with the formula for [Pt_2(H_4tg)$_2$(bpy)$_2$]$(ClO_4)_2$, and the divalent charge of its complex-cation was implied by the molar conductivity in water (191.0 S cm^2 mol^{-1}). The presence of ClO_4^- as a counteranion was indicated by its IR spectrum (Supporting Information, Figure S2), which shows a strong band at 623 cm^{-1} characteristic for ClO_4^-.[23] As in the case of [**1**], the ^1H NMR spectrum of [**2**]$(ClO_4)_2$ in D_2O exhibits aliphatic proton signals in the region δ 3.2–5.0 and aromatic proton signals in the region δ 7.8–8.9 (Supporting Information, Figure S1). However, the integration ratio of the aliphatic and aromatic proton signals is 7:8, indicating that [**2**]$^{2+}$ contains H_4tg^- and bpy ligands in a 1:1 ratio. On the basis of these results, [**2**]$^{2+}$ is assigned to a diplatinum(II) complex, [Pt_2(μ_2-H_4tg-κ^1S:κ^1S)$_2$(bpy)$_2$]$^{2+}$, in which two [Pt(bpy)]$^{2+}$ units are spanned by two H_4tg^- ligands through sulfur bridges.[24,25] This assignment was confirmed by single-crystal X-ray analysis for [**2**]$(ClO_4)_2 \cdot 9H_2O$.

The asymmetric unit of [**2**]$(ClO_4)_2 \cdot 9H_2O$ contains a complex-cation and two perchlorate anions, besides solvated water molecules. The number of perchlorate anions implies that the complex-cation is divalent, consistent with the molar conductivity. As shown in Figure 2, the complex-cation [**2**]$^{2+}$ consists of a [Pt(H_4tg)$_2$(bpy)] unit that chelates to a [Pt(bpy)]$^{2+}$ moiety through thiolato S atoms, forming an S-bridged dinuclear structure in [Pt_2(μ_2-H_4tg-κ^1S:κ^1S)$_2$(bpy)$_2$]$^{2+}$ with a $Pt^{II}{}_2S_2$ diamond core [av S–Pt–S = 82.02(2)°, Pt–S–Pt = 96.8(6)°]. This implies that [Pt(H_4tg-*κS*)$_2$(bpy)] ([**1**]) acts as a bidentate-*S*,*S*′ chelating metalloligand toward a Pt^{II} center. Alternatively, it is considered that this dinuclear structure in [**2**]$^{2+}$ is constructed by the connection of two [Pt(bpy)]$^{2+}$ units with use of two bridging H_4tg^- ligands. Indeed, [**2**]$(ClO_4)_2$ was also obtained by the direct reaction of [$PtCl_2$(bpy)] with NaH_4tg in a 1:1 ratio in water (Scheme 1). Each Pt^{II} atom in [**2**]$^{2+}$ has a square-planar *cis*-N_2S_2 geometry [av N–Pt–N = 79.78(14)°, N–Pt–S = 99.1(15)°], coordinated by a bidentate-*N*,*N*′ bpy and two monodentate-*S* H_4tg^- ligands. The Pt–N [av 2.046(5) Å] and Pt–S [av 2.296(7) Å] bond distances are comparable with the normal Pt–N (av 2.054 Å) and Pt–S (av 2.308 Å) distances for [$Pt^{II}(N)_2(S)_2$]-type complexes.[26] The bond distances and angles about each H_4tg^- ligand are very similar to those found in KH_4tg,[27] having the *β*-D-pyranose ring with the usual chair conformation. Considering the relative

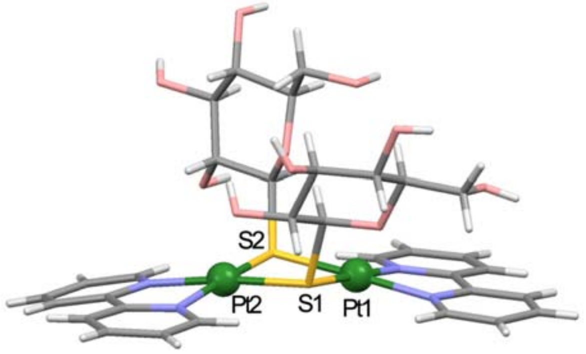

Figure 2. Perspective view of [**2**]$^{2+}$; Pt, green; S, yellow; O, pink; N, blue; C, gray; H, light gray.

arrangement of two β-D-pyranose moieties, two geometrical configurations, syn and anti, are possible for this type of dinuclear complex (Figure 3). As shown in Figure 2, $[\mathbf{2}]^{2+}$ adopts the syn configuration, which appears to be sterically crowded. To avoid the steric repulsion, the two PtN_2S_2 planes are deviated from coplanarity with a dihedral angle of 164.36(4)°. In packing structure, each diplatinum(II) complex-cation is connected to four adjacent complex-cations through intermolecular $\pi-\pi$ interactions between bpy ligands [av C⋯C = 3.34(6) Å], constructing a 2D layer structure with a hydrophilic surface covered with β-D-pyranose moieties and a hydrophobic surface covered with bpy ligands (Supporting Information, Figure S4). These layers are stacked in an $(AB)_n$ fashion such that wide hydrophilic and narrow hydrophobic 2D coordination spaces are alternately formed. There exist interlayer $\pi-\pi$ interactions between bpy ligands in the hydrophobic spaces [av C⋯C = 3.30(3) Å], while hydroxyl groups of β-D-pyranose moieties form hydrogen-bonding networks with ClO_4^- anions and water molecules in the hydrophilic spaces [av $O_{OH}\cdots O_{anion}$ = 2.871(6) Å, $O_{OH}\cdots O_{water}$ = 2.8(2) Å]. It seems that these multiple $\pi-\pi$ and hydrogen-bonding interactions are responsible for the formation of the syn configuration in $[\mathbf{2}]^{2+}$, rather than the anti configuration.

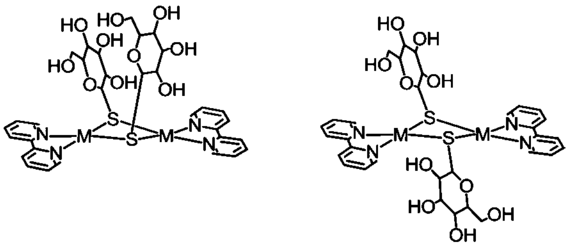

Syn Configuration *Anti* Configuration

Figure 3. Syn and anti configurations for a dinuclear complex.

The absorption spectrum of $[\mathbf{2}](ClO_4)_2$ in water in the near-UV region resembles that of [**1**], showing a bpy $\pi-\pi^*$ transition band at a similar wavelength (Figure 1). In the visible region, however, no clear LL′CT band is observed for $[\mathbf{2}](ClO_4)_2$. This is most likely due to the formation of a μ_2-thiolato structure in $[\mathbf{2}]^{2+}$, which stabilizes the HOMO of the thiolato donor and causes the blue shift of the LL′CT band. In parallel with the absorption spectral feature, $[\mathbf{2}](ClO_4)_2$ does not show any detectable CD bands in the visible region, although several CD bands are observed in the near-UV region (Figure 1).

Synthesis and Characterization of $[PtCu(\mu_2\text{-}H_4tg\text{-}\kappa^1S{:}\kappa^2O,S)_2(bpy)_2]^{2+}$ ($[\mathbf{3}]^{2+}$) and $[PtNi(\mu_2\text{-}H_4tg\text{-}\kappa^1S{:}\kappa^2O,S)_2(bpy)_2]^{2+}$ ($[\mathbf{4}]^{2+}$). To clarify the possible coordination mode of [**1**] toward transition-metal ions that can take both square-planar and octahedral geometries, the reactions of [**1**] with Cu^{2+} and Ni^{2+} in the presence of bpy were studied. Treatment of an aqueous suspension of [**1**] with $[CuCl_2(bpy)]$ in a 1:1 ratio gave a green solution, from which green crystals ($[\mathbf{3}](NO_3)_2$) were isolated in a moderate yield by the addition of an aqueous solution of $NaNO_3$. Similar treatment of $[Pt(H_4tg\text{-}\kappa S)_2(bpy)]$ with a 1:1 mixture of $Ni(NO_3)_2{\cdot}6H_2O$ and bpy in water, followed by the addition of $NaNO_3$, afforded pale green crystals ($[\mathbf{4}](NO_3)_2$). X-ray fluorescence spectrometry indicated the presence of Cu and Ni atoms in $[\mathbf{3}](NO_3)_2$ and $[\mathbf{4}](NO_3)_2$, respectively, besides Pt atoms, and the elemental analytical data of $[\mathbf{3}](NO_3)_2$ and $[\mathbf{4}](NO_3)_2$ were consistent with the formulas for $[PtCu(H_4tg)_2(bpy)_2](NO_3)_2$ and $[PtNi(H_4tg)_2(bpy)_2](NO_3)_2$, respectively. The divalent nature of the complex-cations in $[\mathbf{3}](NO_3)_2$ and $[\mathbf{4}](NO_3)_2$ was implied by their molar conductivities in water {192.7 S cm^2 mol^{-1} for $[\mathbf{3}](NO_3)_2$, 210.2 S cm^2 mol^{-1} for $[\mathbf{4}](NO_3)_2$}, and the presence of NO_3^- as counteranions was indicated by the appearance of an IR band at 1382 cm^{-1} characteristic for NO_3^- (Supporting Information, Figure S2).[23] The $Pt^{II}Cu^{II}$ and the $Pt^{II}Ni^{II}$ dinuclear structures in $[\mathbf{3}]^{2+}$ and $[\mathbf{4}]^{2+}$ were established by single-crystal X-ray crystallography for $[\mathbf{3}](ClO_4)_2{\cdot}2H_2O$ and $[\mathbf{4}](NO_4)_2{\cdot}2H_2O$, respectively.

The asymmetric unit of $[\mathbf{3}](ClO_4)_2{\cdot}2H_2O$ contains a complex-cation and two perchlorate anions, besides solvated water molecules. The number of perchlorate anions implies that the complex-cation is divalent. As shown in Figure 4, the complex-cation $[\mathbf{3}]^{2+}$ consists of a square-planar $[Pt(H_4tg)_2(bpy)]$ unit that chelates to a $[Cu(bpy)]^{2+}$ moiety through thiolato S atoms, forming an S-bridged $Pt^{II}Cu^{II}$ dinuclear structure with a $Pt^{II}Cu^{II}S_2$ diamond core [av S−Pt−S = 84.94(8)°, Pt−S−Cu = 95.8(10)°, S−Cu−S = 83.14(9)°, Pt−S = 2.288(9) Å, Cu−S = 2.33(3) Å]. It is interesting to note that thiolato-bridged dinuclear complexes with a Pt^{II}−S−Cu^{II} linkage have not been reported to date. The bond distances and angles about the Pt^{II} center in $[\mathbf{3}]^{2+}$ [av N−Pt−N = 79.6(4)°, N−Pt−S = 97.8(9)°, Pt−N = 2.052(11) Å], as well as the chair conformational β-D-pyranose ring of H_4tg^-, are very similar to those in $[\mathbf{2}]^{2+}$. In $[\mathbf{3}]^{2+}$, however, two hydroxyl O atoms from two H_4tg^- ligands also bind to a Cu^{II} center at apical positions, with one shorter and the other longer Cu−O distances [Cu1−O2 = 2.386(4) Å, Cu1−O7 = 2.680(6) Å], such that the Cu^{II} atom is situated in a Jahn−Teller distorted octahedral geometry with a *trans*-(*O*)-$N_2O_2S_2$ donor set. This implies that $[Pt(H_4tg\text{-}\kappa S)_2(bpy)]$ acts as a tetradentate-*O*,*O*′,*S*,*S*′ metalloligand toward a Cu^{II} center by using two thiolato and two hydroxyl groups. Unlike in $[\mathbf{2}]^{2+}$, the two H_4tg^- ligands in $[\mathbf{3}]^{2+}$ adopt the anti configuration, which allows the two H_4tg^- ligands to chelate to the Cu^{II} center through thiolato and hydroxyl groups. Of two chiral configurations, Δ and Λ, which arise from the skew pair of a *N*,*N*′-bpy and two *O*,*S*-H_4tg^- chelate rings, the Cu^{II} center in $[\mathbf{3}]^{2+}$ has the Δ configuration. This chiral configuration regulates the two asymmetric bridging S atoms of H_4tg^- to have the *R* configuration. The five-membered *O*,*S*-chelate rings of H_4tg^- adopt a gauche form with the λ

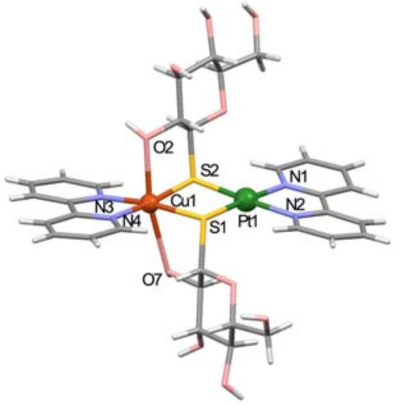

Figure 4. Perspective view of $[\mathbf{3}]^{2+}$; Pt, green; Cu, brown; S, yellow; O, pink; N, blue; C, gray; H, light gray.

conformation that is thermodynamically stable.[28] Molecular model examinations reveal that the two *O,S*-chelate rings are enforced to have an unfavorable envelope form when the Cu^{II} center has the Λ configuration. Moreover, there exists a nonbonding interaction between a C2 proton of H_4tg^- and a bpy aromatic ring of $[Pt(bpy)]^{2+}$ in the Λ configuration. The selection of the Δ configuration in $[\mathbf{3}]^{2+}$ is most likely ascribed to these steric factors that are caused by the presence of the rigid, bulky H_4tg^- ligands with the *β*-D-pyranose ring. In packing structure, the complex-cations $[\mathbf{3}]^{2+}$ are connected with each other through intermolecular *π*−*π* interactions [av C⋯C = 3.45(10) Å] between bpy ligands, forming a 2D sheetlike structure (Supporting Information, Figure S5). The 2D sheets are further connected by intermolecular hydrogen bonds between hydroxyl groups of H_4tg^- [av O⋯O = 2.748(3) Å], which completes a 3D network structure.

The asymmetric unit of $[\mathbf{4}](NO_3)_2{\cdot}2H_2O$ contains a complex-cation and two nitrate anions, besides solvated water molecules. The number of nitrate anions implies that the complex-cation is divalent. As shown in Figure 5, the complex cation $[\mathbf{4}]^{2+}$ consists of a square-planar $[Pt(H_4tg)_2(bpy)]$ unit that binds to a $[Ni(bpy)]^{2+}$ moiety through two thiolato S and two hydroxyl O atoms from two H_4tg^- ligands, forming an S-bridged $Pt^{II}Ni^{II}$ dinuclear structure in $[PtNi(\mu_2\text{-}H_4tg\text{-}\kappa^1S{:}\kappa^2O,S)_2(bpy)_2]^{2+}$ with a $Pt^{II}Ni^{II}S_2$ diamond core [av S−Pt−S = 86.40(4)°, Pt−S−Ni = 96.0(1)°, S−Ni−S = 80.71(4)°, Pt−S = 2.30(2) Å, Ni−S = 2.43(3) Å]. The overall dinuclear structure in $[\mathbf{4}]^{2+}$ with anti configurational H_4tg^- ligands corresponds well with that in $[\mathbf{3}]^{2+}$, except for the presence of Ni^{II} atom in place of Cu^{II} atom. In particular, the bond distances and angles about the Pt^{II} atom in $[\mathbf{4}]^{2+}$ [av N−Pt−N = 79.69(15)°, N−Pt−S = 97(2)°, Pt−N = 2.058(1) Å] are very similar to those in $[\mathbf{3}]^{2+}$. The Ni−S bond distances in $[\mathbf{4}]^{2+}$ are longer than the Cu−S distances in $[\mathbf{3}]^{2+}$, while the Ni−O bond distances in $[\mathbf{4}]^{2+}$ [2.139(3) Å, 2.145(3) Å] are much shorter than the Cu−O distances in $[\mathbf{3}]^{2+}$. In addition, the O−Ni−O angle in $[\mathbf{4}]^{2+}$ [176.77(12)°] is very close to 180°, compared with the O−Cu−O angle in $[\mathbf{3}]^{2+}$ [166.83(15)°]. Thus, the Ni^{II} atom in $[\mathbf{4}]^{2+}$ has an octahedral geometry more ideal than the Cu^{II} atom in $[\mathbf{3}]^{2+}$, which is understood by the absence of the Jahn−Teller distortion for a d^8 metal center. Like the Cu^{II} center in $[\mathbf{3}]^{2+}$, the Ni^{II} center in $[\mathbf{4}]^{2+}$ is chelated by a bidentate-*N,N′* bpy and two bidentate-*O,S* H_4tg^- ligands to have the Δ configuration, with two bridging S atoms being fixed to the *R* configuration. A related S-bridged $Pt^{II}Ni^{II}$ dinuclear complex with two terminal bpy ligands, $[PtNi(\mu_2\text{-aet-}\kappa^1S{:}\kappa^2S,N)_2(bpy)_2]^{2+}$ (aet = 2-aminoethanethiolate), has been reported, although a pair of enantiomers (Δ_{RR}/Λ_{SS}) with the Δ/Δ configurational Ni center and the *R*/*S* configurational S center is formed in this structure because of the use of achiral aet ligands.[29] In the packing structure, the complex-cations are connected with each other through intermolecular *π*−*π* interactions to form a 1D chain [av C⋯C = 3.48(12) Å] in $[\mathbf{4}](NO_3)_2{\cdot}2H_2O$, and the 1D chains are further connected by intermolecular hydrogen bonds between hydroxyl groups of H_4tg^- [av O⋯O = 3.0(2) Å] to complete a 3D network structure (Supporting Information, Figure S6).

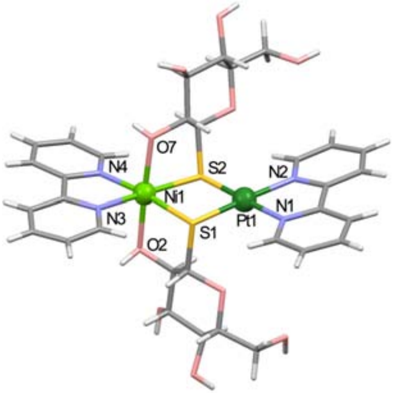

Figure 5. Perspective view of $[\mathbf{4}]^{2+}$; Pt, green; Ni, yellow-green; S, yellow; O, pink; N, blue; C, gray; H, light gray.

The absorption spectrum of $[\mathbf{3}](NO_3)_2$ in water is characterized by a weak visible band at 616 nm ($\varepsilon = 4.2 \times 10^2$ M^{-1} cm^{-1}), which is typical for a d−d transition band found in Cu^{II} species,[30] besides an intense near-UV band at 310 nm ($\varepsilon = 2.61 \times 10^4$ M^{-1} cm^{-1}) due to a bpy *π*−*π** transition (Figure 6). This absorption spectral feature is essentially the same as that of its diffuse reflection spectrum in the solid state (Supporting Information, Figure S7). In addition, the CD spectrum of $[\mathbf{3}](NO_3)_2$ in water gives a negative CD band at 603 nm ($\Delta\varepsilon = -3.33$ M^{-1} cm^{-1}) in the visible d−d band region, which is also found in its CD spectrum in the solid state. Thus, it is reasonable to assume that the S-bridged $Pt^{II}Cu^{II}$ dinuclear structure in $[\mathbf{3}]^{2+}$ is retained in water, although a partial Cu−O bond cleavage may not be ruled out.

When $[\mathbf{4}](NO_3)_2$ is dissolved in water, its absorption and CD spectra do not give any detectable band in the visible region, and their spectral features are very similar to those of [**1**] ($[Pt(H_4tg\text{-}\kappa S)_2(bpy)]$) over the whole region (Figure 6). In the solid state, $[\mathbf{4}](NO_3)_2$ exhibits a characteristic weak visible band (574 nm) assignable to a d−d transition for an octahedral Ni^{II} center[31] and a negative CD band (569 nm) in this d−d band region (Supporting Information, Figure S8). Thus, it is considered that the S-bridged $Pt^{II}Ni^{II}$ structure of $[\mathbf{4}]^{2+}$ found in the crystal is decomposed into the mononuclear [**1**] and aqua Ni^{II} species in water. This seems to be related to the longer Ni−S bonds in $[\mathbf{4}]^{2+}$, which facilitates the cleavage of Ni−S bonds in water. On the other hand, the absorption spectrum of $[\mathbf{4}]^{2+}$ in methanol shows a weak d−d band at 571 nm ($\varepsilon = 29$ M^{-1} cm^{-1}), besides a bpy *π*−*π** transition band at 305 nm ($\varepsilon = 2.7 \times 10^4$ M^{-1} cm^{-1}) (Figure 6). In addition, a negative CD band is observed in the d−d band region (568 nm), as in the case of the CD spectrum in the solid state. This is suggestive of the retention of the S-bridged $Pt^{II}Ni^{II}$ dinuclear structure in methanol, which is understood by a weaker coordination ability of MeOH compared with that of H_2O.

Synthesis and Characterization of $[Cd\{Pt(\mu_2\text{-}H_4tg\text{-}\kappa^1S{:}\kappa^2O,S)(\mu_2\text{-}H_4tg\text{-}\kappa^1S{:}\kappa^1S)(bpy)\}_2]^{2+}$ ($[\mathbf{5}]^{2+}$). We also investigated the coordination ability of [**1**] toward thiophilic Cd^{2+}, which can take various coordination geometries, including tetrahedron and octahedron. When $[Pt(H_4tg\text{-}\kappa S)_2(bpy)]$ was treated with a 1:1 mixture of $CdCl_2{\cdot}2.5H_2O$ and bpy in water, we obtained a yellow reaction solution, from which yellow block crystals ($[\mathbf{5}](ClO_4)_2$) were isolated by the addition of $NaClO_4$. Compound $[\mathbf{5}](ClO_4)_2$ is almost insoluble in any common solvents, including water and alcohol, and thus, its characterization in solution could not be carried out. The presence of bpy and H_4tg^- ligands in $[\mathbf{5}](ClO_4)_2$, besides ClO_4^- ions, was confirmed by the IR spectrum that is similar to the spectrum of $[\mathbf{2}](ClO_4)_2$ (Supporting Information, Figure S2), the diffuse reflection spectrum that shows characteristic *π*−*π** transition bands centered at 325 nm, and the solid-state

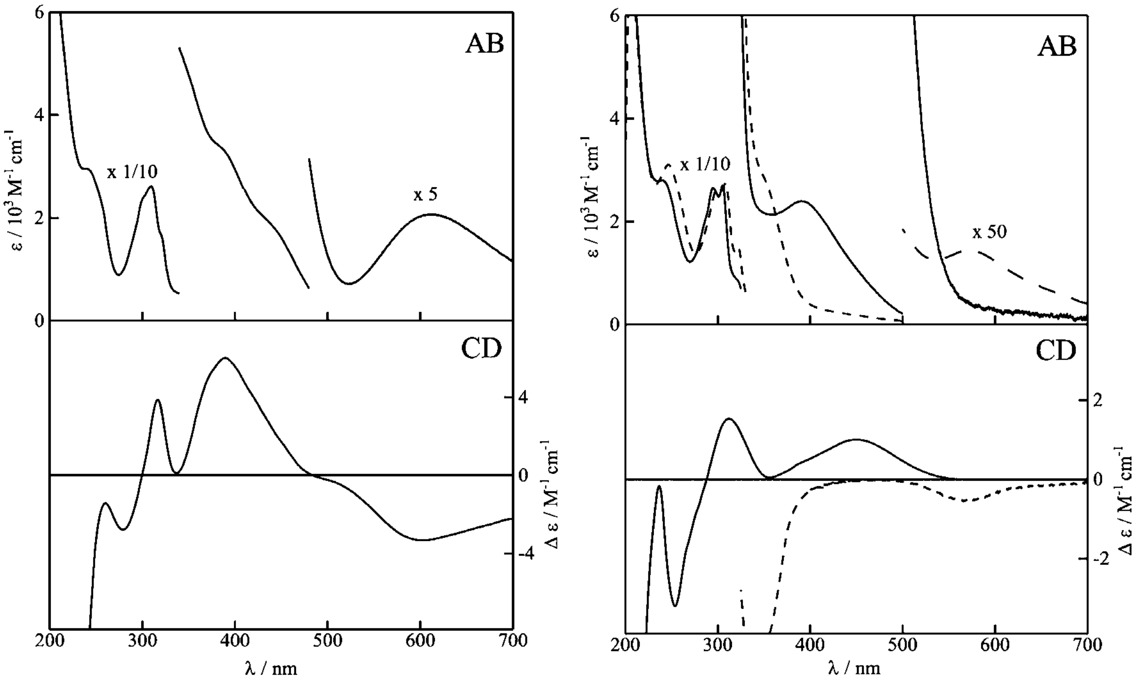

Figure 6. Absorption and CD spectra of complexes $[\mathbf{3}](NO_3)_2$ (left) and $[\mathbf{4}](NO_3)_2$ (right) in H_2O (solid line) and MeOH (dashed line).

CD spectrum that gives a negative band at 341 nm (Supporting Information, Figure S9). However, the elemental analytical data for $[\mathbf{5}](ClO_4)_2$ is not in agreement with a formula for an expected $Pt^{II}Cd^{II}$ dinuclear complex but for a $Pt^{II}Cd^{II}Pt^{II}$ trinuclear complex, $[Cd\{Pt(H_4tg)_2(bpy)\}_2](ClO_4)_2$. In addition, X-ray fluorescence spectrometry implies the presence of Pt and Cd atoms in a 2:1 ratio in $[\mathbf{5}](ClO_4)_2$, rather than in a 1:1 ratio. These results indicate that $[\mathbf{5}]^{2+}$ contains $[Pt(H_4tg)_2(bpy)]$ and Cd^{II} in a 2:1 ratio, with the lack of an additional bpy ligand bound to a Cd^{II} center. Consistent with this, yellow block crystals of $[\mathbf{5}](ClO_4)_2$ were obtained in a reasonable yield by the 2:1 reaction of $[\mathbf{1}]\cdot 2H_2O$ with $CdBr_2$ in water, followed by the addition of $NaClO_4$, without the addition of bpy to the reaction mixture. The $Pt^{II}Cd^{II}Pt^{II}$ trinuclear structure in $[\mathbf{5}]^{2+}$ was unambiguously determined by single-crystal X-ray analysis for $[\mathbf{5}](ClO_4)_2\cdot 6H_2O$.

As shown in Figure 7, the complex cation consists of two square-planar $[Pt(H_4tg)_2(bpy)]$ units and one Cd^{II} atom. Each of two $[Pt(H_4tg)_2(bpy)]$ units chelates to the Cd^{II} atom through two thiolato S atoms [av Cd−S = 2.65(4) Å, S1−Cd−S1 = 93.42(8)°, S1−Cd−S2 = 75.00(5)°, S2−Cd−S2 = 118.82(8)°], forming an S-bridged $Pt^{II}Cd^{II}Pt^{II}$ trinuclear structure with a crystallographic C_2 symmetry. An interesting structural feature of $[\mathbf{5}]^{2+}$ is the coordination of a hydroxyl group from one of two H_4tg^- ligands in each $[Pt(H_4tg)_2(bpy)]$ unit [Cd−O = 2.446(5) Å], such that the Cd^{II} center is situated in a highly distorted octahedral geometry with a *trans*-(*O*)-O_2S_4 donor set [O−Cd−O = 145.0(2)°, trans S−Cd−S = 163.08(6)°]. Thus, $[\mathbf{5}]^{2+}$ is formulated as $[Cd\{Pt(\mu_2\text{-}H_4tg\text{-}\kappa^1S{:}\kappa^2O,S)(\mu_2\text{-}H_4tg\text{-}\kappa^1S{:}\kappa^1S)(bpy)\}_2]^{2+}$, in which each $[Pt(H_4tg)_2(bpy)]$ unit acts as a tridentate-*O*,*S*,*S′* metalloligand. This coordination mode of $[Pt(H_4tg)_2(bpy)]$ is distinct from the modes found in $[\mathbf{2}]^{2+}$, $[\mathbf{3}]^{2+}$, and $[\mathbf{4}]^{2+}$, although the bond distances and angles about the $[Pt(H_4tg)_2(bpy)]$ unit [av S−Pt−S = 89.56(7)°, N−Pt−N = 78.9(2)°, trans N−Pt−S = 173(2)°, Pt−S = 2.293(4) Å, Pt−N = 2.076(6) Å] are very similar. Like in $[\mathbf{3}]^{2+}$ and $[\mathbf{4}]^{2+}$, the four bridging S atoms in $[\mathbf{5}]^{2+}$ adopt the *R* configuration, and the two *O*,*S*-chelate rings of H_4tg^- have a gauche form with the λ conformation. However, the Cd center in $[\mathbf{5}]^{2+}$ is regulated to have the Λ configuration, which is opposite to the Δ configurational Cu^{II} and Ni^{II} centers in $[\mathbf{3}]^{2+}$ and $[\mathbf{4}]^{2+}$. Thus, the bis(*O*,*S*-chelation) mode to an octahedral metal center from two $[Pt(H_4tg)_2(bpy)]$ units leads to the chiral configuration opposite to that formed by the bis(*O*,*S*-chelation) mode from one $[Pt(H_4tg)_2(bpy)]$ unit. Molecular model examinations indicate that the *O*,*S*-chelate rings are enforced to have an unfavorable envelope form when the Cd^{II} center adopts the Δ configuration. Moreover, there exists a nonbonding interaction between a C2 proton of H_4tg^- and a lone-pair on a bridging S atom from a different $[Pt(H_4tg)_2(bpy)]$ unit in the Δ configuration. Notable are the existing intramolecular hydrogen bonds between hydroxyl groups of H_4tg^- from different $[Pt(H_4tg)_2(bpy)]$ units in $[\mathbf{5}]^{2+}$ [av O···O = 2.68(5) Å], which appear to sustain the $Pt^{II}Cd^{II}Pt^{II}$ trinuclear structure with the Δ configurational Cd^{II} center. In packing structure, each complex-cation $[\mathbf{5}]^{2+}$ is

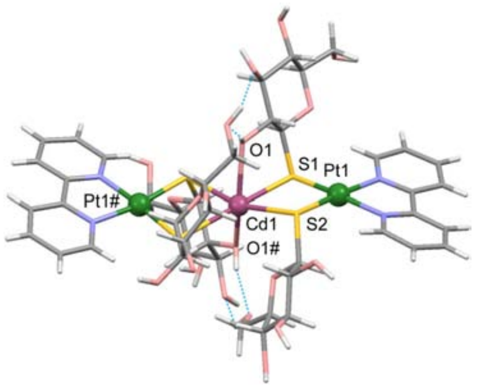

Figure 7. Perspective view of $[\mathbf{5}]^{2+}$; Pt, green; Cd, purple; S, yellow; O, pink; N, blue; C, gray; H, light gray. Dashed lines indicate O−H···O hydrogen bonds.

hydrogen bonded with six adjacent complex-cations through hydroxyl groups of H_4tg^- [av O⋯O = 2.78(5) Å], constructing a 3D network structure (Supporting Information, Figure S10). The 3D network structure is reinforced by hydrogen bonds between hydroxyl groups of H_4tg^- and ClO_4^- ions [av O⋯O = 2.91(3) Å]. It is considered that these multiple hydrogen-binding interactions are responsible for the insolubility of $[\mathbf{5}](ClO_4)_2$ in any common solvents.

■ CONCLUDING REMARKS

In this study, we showed that Cl^- ions in $[PtCl_2(bpy)]$ are readily replaced by H_4tg^- in water to form the mononuclear $[Pt(H_4tg\text{-}\kappa S)_2(bpy)]$ ([**1**]). Compound [**1**] further reacted with $[PtCl_2(bpy)]$ to give the diplatinum(II) complex, $[Pt_2(\mu_2\text{-}H_4tg\text{-}\kappa^1 S{:}\kappa^1 S)_2(bpy)_2]^{2+}$ ($[\mathbf{2}]^{2+}$), in which two $[Pt(bpy)]^{2+}$ moieties are spanned by two H_4tg^- ligands through thiolato S atoms. This result indicates that [**1**] functions as a bidentate-*S*,*S′* metalloligand toward a square-planar metal center due to the high nucleophilicity of H_4tg^- thiolato groups bound to a Pt^{II} center. Interestingly, [**1**] was found to serve as a tetradentate-*O*,*O′*,*S*,*S′* metalloligand to M = Cu^{II}, Ni^{II} in the presence of bpy, affording the heterometallic dinuclear structures in $[PtCu(\mu_2\text{-}H_4tg\text{-}\kappa^1 S{:}\kappa^2 O,S)_2(bpy)_2]^{2+}$ ($[\mathbf{3}]^{2+}$) and $[PtNi(\mu_2\text{-}H_4tg\text{-}\kappa^1 S{:}\kappa^2 O,S)_2(bpy)_2]^{2+}$ ($[\mathbf{4}]^{2+}$), which contain an octahedral metal center bound by two thiolato and two hydroxyl groups, besides a bpy ligand. While several metal complexes with H_4tg^- or H_3tg^{2-} have been reported,[5−10] coordination of a hydroxyl group toward a metal center has not been recognized.[32] A similar reaction with Cd^{2+} led to the formation of the $Pt^{II}Cd^{II}Pt^{II}$ trinuclear complex, $[Cd\{Pt(\mu_2\text{-}H_4tg\text{-}\kappa^1 S{:}\kappa^2 O,S)(\mu_2\text{-}H_4tg\text{-}\kappa^1 S{:}\kappa^1 S)(bpy)\}_2]^{2+}$ ($[\mathbf{5}]^{2+}$), in which each of two molecules of [**1**] binds to an octahedral Cd^{II} center in a tridentate-*O*,*S*,*S′* mode. Thus, the present study showed that [**1**] functions as a versatile multidentate metalloligand, the coordination modes of which are varied with response to the coordination environment of a metal center. Of two geometrical configurations, syn and anti, $[\mathbf{2}]^{2+}$ adopted the syn configuration so as to form both of the intermolecular O−H⋯O hydrogen bonds between hydroxyl groups of H_4tg^- and the intermolecular $\pi-\pi$ interactions between bpy ligands. On the other hand, $[\mathbf{3}]^{2+}$, $[\mathbf{4}]^{2+}$, and $[\mathbf{5}]^{2+}$ selected the anti configuration, which permits H_4tg^- in [**1**] to chelate to a metal center through thiolato and hydroxyl groups to complete an octahedral geometry. The most remarkable structural feature in the present system is the formation of the Δ configurational metal center in $[\mathbf{3}]^{2+}$ and $[\mathbf{4}]^{2+}$ and the Λ configurational metal center in $[\mathbf{5}]^{2+}$, indicative of the availability of [**1**] as the chiralselective construction of S-bridged multinuclear structures. This is explained by the steric demand around an octahedral metal center, which is regulated by the coordination of chiral H_4tg^- with a rigid, bulky *β*-D-pyranose ring. It is worth mentioning that the $Pt^{II}Cu^{II}$ structure in $[\mathbf{3}]^{2+}$ is retained in water, while the $Pt^{II}Ni^{II}$ structure in $[\mathbf{4}]^{2+}$ is decomposed into [**1**] in water, although $[\mathbf{4}]^{2+}$ is fairly stable in methanol. The difference in stability between $[\mathbf{3}]^{2+}$ and $[\mathbf{4}]^{2+}$ in water is most likely ascribed to the stronger Cu−S bonds in $[\mathbf{3}]^{2+}$, which is induced by the Jahn−Teller elongation of axial Cu^{II}−O bonds. Finally, it should be noted that only a few transition-metal complexes with H_4tg^- or H_3tg^{2-} have been isolated and crystallographically characterized to date.[9,10] The successful preparation and structural determination of all the multinuclear complexes obtained in this work are thanks to the use of the chiral metalloligand with H_4tg^-, which leads to the stereoselective formation of a single isomer for each complex, as well as thanks to the introduction of a hydrophobic coligand of bpy in the hydrophilic H_4tg^- system. A similar strategy could be applicable for the isolation and structural characterization of other monosaccharide coordination systems.

■ ASSOCIATED CONTENT

Ⓢ Supporting Information

X-ray crystallographic files in CIF format for all complexes, crystallographic data, selected bond distances and angles, and figures of IR, solid-state diffuse reflection, CD, ESI-mass, and NMR spectra. This material is available free of charge via the Internet at http://pubs.acs.org.

■ AUTHOR INFORMATION

Corresponding Author

*E-mail: konno@chem.sci.osaka-u.ac.jp.

Notes

The authors declare no competing financial interest.

■ ACKNOWLEDGMENTS

This work was partly supported by a Grant-in-Aid for Science Research No. 23350026 from the Ministry of Education, Culture, Sports, Science and Technology of Japan.

■ REFERENCES

(1) (a) Horton, D.; Hutson, D. H. *Adv. Carbohydr. Chem.* **1963**, *18*, 123−199. (b) Schmidt, R. R. *Angew. Chem., Int. Ed. Engl.* **1986**, *25*, 212−235.

(2) (a) Fuhrhop, J.-H.; David, H.-H.; Mathieu, J.; Liman, U.; Winter, H.-J.; Boekema, E. *J. Am. Chem. Soc.* **1986**, *108*, 1785−1791. (b) Zhu, Y.; van der Donk, W. A. *Org. Lett.* **2001**, *3*, 1189−1192. (c) Cohen, S. B.; Halcomb, R. L. *J. Am. Chem. Soc.* **2001**, *124*, 2534−2543. (d) Galonić, D. P.; Ide, N. D.; van der Donk, W. A.; Gin, D. Y. *J. Am. Chem. Soc.* **2005**, *127*, 7359−7369. (e) Floyd, N.; Vijayakrishnan, B.; Koeppe, J. R.; Davis, B. G. *Angew. Chem., Int. Ed.* **2009**, *48*, 7798−7802. (f) Fiore, M.; Conte, M. L.; Pacifico, S.; Marra, A.; Dondoni, A. *Tetrahedron Lett.* **2011**, *52*, 444−447.

(3) (a) Ackerson, C. J.; Jadzinsky, P. D.; Kornberg, R. D. *J. Am. Chem. Soc.* **2005**, *127*, 6550−6551. (b) Watanabe, S.; Yoshida, K.; Shinkawa, K.; Kumagawa, D.; Seguchi, H. *Colloids Surf. B* **2010**, *81*, 570−577. (c) Kycia, A. H.; Wang, J.; Merrill, A. R.; Lipkowski, J. *Langmuir* **2011**, *27*, 10867−10877. (d) Kycia, A. H.; Sek, S.; Su, Z.; Merrill, A. R.; Lipkowski, J. *Langmuir* **2011**, *27*, 13383−13389.

(4) Shaw, C. F., III *Chem. Rev.* **1999**, *99*, 2589−2600.

(5) (a) Landé, K. *Muench. Med. Wochenschr.* **1927**, *74*, 1132−1134. (b) Pick, E. *Wien. Klin. Wochnschr.* **1927**, *40*, 1175−1176. (c) Forestier, J. *J. Lab. Clin. Med.* **1935**, *20*, 827−840. (d) Shaw, C. F., III; Eldridge, J.; Cancro, M. P. *J. Inorg. Biochem.* **1981**, *14*, 267−274. (e) Brown, K.; Parish, R. V.; McAuliffe, C. A. *J. Am. Chem. Soc.* **1981**, *103*, 4943−4945. (f) Hill, D. T.; Sutton, B. M.; Isab, A. A.; Razi, T.; Sadler, P. J.; Trooster, J. M.; Calis, G. H. M. *Inorg. Chem.* **1983**, *22*, 2936−2942. (g) Hu, M.-L.; Dillard, C. J.; Tappel, A. L. *Agents Actions* **1988**, *25*, 132−138. (h) Isab, A. A. *J. Inorg. Biochem.* **1992**, *46*, 145−151.

(6) (a) Tepperman, K.; Finer, R.; Donovan, S.; Elder, R. C.; Doi, J.; Ratliff, D.; Ng, K. *Science* **1984**, *225*, 430−432. (b) Berners-Price, S. J.; Jarrett, P. S.; Sadler, P. J. *Inorg. Chem.* **1987**, *26*, 3074−3077.

(7) (a) Ferrier, R. J.; Furneaux, R. H. *Carbohydr. Res.* **1977**, *57*, 73−83. (b) Oh, S. J.; Ryu, J.-S.; Yoon, E.-J.; Bae, M. S.; Choi, S. J.; Park, K. B.; Moon, D. H. *Appl. Radiat. Isot.* **2006**, *64*, 207−215.

(8) (a) Becker, K.; Herold-Mende, C.; Park, J. J.; Lowe, G.; Schirmer, R. H. *J. Med. Chem.* **2001**, *44*, 2784−2792. (b) Gottschaldt, M.; Pfeifer, A.; Koth, D.; Görls, H.; Dahse, H.-M.; Möllmann, U.; Obata, M.; Yano, S. *Tetrahedron* **2006**, *62*, 11073−11080. (c) Fontana, G.; Abbate, M.; Casella, G.; Pellerito, C.; Longo, A.; Ferrante, F. *Polyhedron* **2011**, *30*, 1671−1679.

(9) Okamoto, K.-I.; Arashi, K.; Hidaka, J.; Konno, T. *Bull. Chem. Soc. Jpn.* **1994**, *67*, 2736−2743.

(10) (a) Spies, H.; Johannsen, B. *Analyst* **1995**, *120*, 775−777. (b) Leipnitz, P.; Reck, G.; Pietzsch, H.-J.; Spies, H. *Forschungszent. Rossendorf* **2001**, *311*, 102−103.

(11) Levy, D. E.; Fuegedi, P. *The Organic Chemistry of Sugars*; CRC Press/Taylor & Francis: Boca Raton, FL, 2006.

(12) (a) Okamoto, K.-I.; Sasaki, C.; Yamada, Y.; Konno, T. *Bull. Chem. Soc. Jpn.* **1999**, *72*, 1685−1696. (b) Konno, T. *Bull. Chem. Soc. Jpn.* **2004**, *77*, 627−649. (c) Igashira-Kamiyama, A.; Konno, T. *Dalton Trans.* **2011**, *40*, 7249−7263.

(13) (a) Toyota, A.; Yamaguchi, T.; Igashira-Kamiyama, A.; Kawamoto, T.; Konno, T. *Angew. Chem., Int. Ed.* **2005**, *44*, 1088−1092. (b) Taguchi, M.; Igashira-Kamiyama, A.; Kajiwara, T.; Konno, T. *Angew. Chem., Int. Ed.* **2007**, *46*, 2422−2425. (c) Hashimoto, Y.; Tsuge, K.; Konno, T. *Chem. Lett.* **2010**, *39*, 601−603. (d) Lee, R.; Igashira-Kamiyama, A.; Motoyoshi, H.; Konno, T. *CrystEngComm* **2012**, *14*, 1936−1938.

(14) (a) Sameshima, Y.; Yoshinari, N.; Tsuge, K.; Igashira-Kamiyama, A.; Konno, T. *Angew. Chem., Int. Ed.* **2009**, *48*, 8469−8472. (b) Yoshinari, N.; Igashira-Kamiyama, A.; Konno, T. *Chem.—Eur. J.* **2010**, *16*, 14247−14251. (c) Yoshinari, N.; Konno, T. *Dalton Trans.* **2011**, *40*, 12191−12200.

(15) (a) Konno, T.; Shimazaki, Y.; Yamaguchi, T.; Ito, T.; Hirotsu, M. *Angew. Chem., Int. Ed.* **2002**, *41*, 4711−4715. (b) Igashira-Kamiyama, A.; Fujioka, J.; Kodama, T.; Kawamoto, T.; Konno, T. *Chem. Lett.* **2006**, *35*, 522−523. (c) Igashira-Kamiyama, A.; Fujioka, J.; Mitsunaga, S.; Nakano, M.; Kawamoto, T.; Konno, T. *Chem.—Eur. J.* **2008**, *14*, 9512−9515. (d) Yoshinari, N.; Tatsumi, K.; Igashira-Kamiyama, A.; Konno, T. *Chem.—Eur. J.* **2010**, *16*, 14252−14255.

(16) (a) Konno, T.; Yoshimura, T.; Aoki, K.; Okamoto, K.-I.; Hirotsu, M. *Angew. Chem., Int. Ed.* **2001**, *40*, 1765−1768. (b) Matsumoto, Z.; Aridomi, T.; Igashira-Kamiyama, A.; Kawamoto, T.; Konno, T. *Inorg. Chem.* **2007**, *46*, 2968−2970. (c) Aridomi, T.; Takamura, K.; Igashira-Kamiyama, A.; Konno, T. *Chem.—Eur. J.* **2008**, *14*, 7752−7755. (d) Aridomi, T.; Igashira-Kamiyama, A.; Konno, T. *Inorg. Chem.* **2008**, *47*, 10202−10204. (e) Saito, K.; Sarukawa, Y.; Tsuge, K.; Konno, T. *Eur. J. Inorg. Chem.* **2010**, 3909−3913.

(17) Janiak, C. *J. Chem. Soc., Dalton Trans.* **2000**, 3885−3896.

(18) Morgan, G. T.; Burstall, F. H. *J. Chem. Soc.* **1934**, 965−971.

(19) (a) Spodine, E.; Atria, A. M.; Calvo, V.; Manzur, J.; Garland, M. T.; Peña, O.; Sergent, M. *J. Chem. Soc., Dalton Trans.* **1991**, *10*, 2707−2710. (b) Hernández-Molina, M.; González-Platas, J.; Ruiz-Pérez, C.; Lloret, F.; Julve, M. *Inorg. Chim. Acta* **1999**, *284*, 258−265.

(20) Sheldrick, G. M. *Acta Crystallogr.* **2008**, *A64*, 112−122.

(21) (a) Gidney, P. M.; Gillard, R. D.; Heaton, B. T. *J. Chem. Soc., Dalton Trans.* **1973**, 132−134. (b) Miskowski, V. M.; Houlding, V. H. *Inorg. Chem.* **1989**, *28*, 1529−1533. (c) Cummings, S. D.; Eisenberg, R. *J. Am. Chem. Soc.* **1996**, *118*, 1949−1960. (d) Connick, W. B.; Gray, H. B. *J. Am. Chem. Soc.* **1997**, *119*, 11620−11627. (e) Yersin, H.; Humbs, W.; Strasser, J. *Coord. Chem. Rev.* **1997**, *159*, 325−358.

(22) (a) Vogler, A.; Kunkely, H. *J. Am. Chem. Soc.* **1981**, *103*, 1559−1660. (b) Zuleta, J. A.; Burberry, M. S.; Eisenberg, R. *Coord. Chem. Rev.* **1990**, *97*, 47−64. (c) Bevilacqua, J. M.; Zuleta, J. A.; Eisenberg, R. *Inorg. Chem.* **1993**, *32*, 3689−3693. (d) Bevilacqua, J. M.; Eisenberg, R. *Inorg. Chem.* **1994**, *33*, 2913−2923. (e) Cummings, S. D.; Eisenberg, R. *Inorg. Chem.* **1995**, *34*, 2007−2014. (f) Paw, W.; Lachicotte, R. J.; Eisenberg, R. *Inorg. Chem.* **1998**, *37*, 4139−4141.

(23) Nakamoto, K. *Infrared and Raman Spectra of Inorganic and Coordination Compounds*, 5th ed.; Wiley Interscience: Chichester, 1997.

(24) The retention of the C_2 symmetrical diplatinum(II) structure in [**2**]$^{2+}$ in solution is supported by its ^{13}C NMR spectrum in D_2O, which shows only a single set of 16 carbon signals (Supporting Information, Figure S1). The ^{13}C NMR spectrum of the other diamagnetic [**1**], which is a neutral species, could not be measured because of its poor solubility.

(25) In the ESI mass spectrum in MeOH, [**2**]$(ClO_4)_2$ dominantly showed a cluster of signals at m/z = 546.1 corresponding to $[Pt_2(H_4tg)_2(bpy)_2]^{2+}$ (Supporting Information, Figure S3). The ESI mass spectra of [**3**]$(ClO_4)_2$ and [**4**]$(NO_3)_2$ displayed main signals at m/z = 764.1 corresponding to $\{[Pt(H_4tg)_2(bpy)]^{+}Na\}^{+}$, suggestive of the dissociation of [**3**]$^{2+}$ and [**4**]$^{2+}$ into the mononuclear [**1**] under a very dilute MeOH solution. The ESI mass spectra of [**1**] and [**5**]$(ClO_4)_2$ could not be measured because of their insolubility in MeOH.

(26) The averaged Pt−N and Pt−S coordination bonds were evaluated on the basis of 275 crystal structures with $R < 0.075$ from the December 2012 version of the Cambridge Crystallographic Database.

(27) Yoshinari, N.; Kitani, N.; Konno, T. *Acta Crystallogr.* **2012**, *C68*, m363−m366.

(28) (a) Corey, E. J.; Bailar, J. C., Jr. *J. Am. Chem. Soc.* **1959**, *81*, 2620−2629. (b) Niketić, S. R.; Rasmussen, K. *Acta Chem. Scand.* **1978**, *A32*, 391−400. (c) Nakashima, T.; Mishiro, J.; Ito, M.; Kura, G.; Ikuta, Y.; Matsumoto, N.; Nakajima, K.; Kojima, M. *Inorg. Chem.* **2003**, *42*, 2323−2330.

(29) (a) Konno, T.; Yoshinari, Y.; Okamoto, K.-I. *Chem. Lett.* **1995**, 989−990. (b) Okamoto, K.-I.; Yoshinari, Y.; Yamada, Y.; Sakagami, N.; Konno, T. *Bull. Chem. Soc. Jpn.* **1998**, *71*, 1363−1371.

(30) Lever, A. B. P. *Inorganic Electronic Spectroscopy*, 2nd ed.; Elsevier: Amsterdam, 1984.

(31) (a) Nicholls, D. *Comprehensive Inorganic Chemistry*; Bailar, J. C., Emeleus, H. J., Nyholm, R., Trotman-Dickenson, A. F., Eds.;Pergamon: Oxford, 1973; Vol. 3. (b) Sacconi, L.; Mani, F.; Bencini, A. *Comprehensive Coordination Chemistry*; Wilkinson, G., Gillard, R., McCleverty, J. A., Eds.; Pergamon: Oxford, 1987; Vol. 5.

(32) A ruthenium(II) complex with H_4tg^- has recently been reported. However, its structural characterization has not been made, and the coordination of a hydroxyl group to a metal center has not been established. See ref 8c.